CHAPTER-VII

INTERACTIONS BETWEEN AN ANTIFUNGAL SULFA DRUG AND DIVERSE MACROCYCLIC POLYETHERS EXPLAINING MECHANISM, PERFORMANCE AND PHYSIOGNOMIES LEADING TO FORMATION OF STABLE COMPLEXES

VII.1. INTRODUCTION

Crown ethers are macrocyclic ligands discovered by Pedersen 1967 [1-3]. Crown ethers are one of the most widely studied family of host compounds in the field of supramolecular chemistry, involving non-covalent interactions.The important characteristics of crown ethers are the number and type of donor atoms, the dimension of the macrocyclic cavity and the preorganization of the host molecule for most effective coordination. Macrocyclic compounds can form complexes with inorganic cations, organic cations and organic neutral molecules in their cavity via different types of interactions with multiple oxygen atoms [4, 5]. Applications of CEs as drug carriers [6] has been in progress on the basis of their inclusion ability. Crown ethers have proved to be unique cyclic molecules for molecular recognition of suitable substrates by hydrogen bonds, ionic interactions and hydrophobic interactions. The study of interactions involved in the complex formation is important for a better understanding of the mechanism of biological transport, molecular recognition, and other analytical applications [7]. They also have medical applications as diagnostic or therapeutic agents [8, 9].

Sulfonamides are considered as an important group of drugs which are used widely as antimicrobial, high ceiling diuretics, anti-thyroid and anti-inflammatory agents [10]. Sulfanilamide, 4-aminobenzenesulfonamide, is the simplest representative in the group of sulfonamide drugs [11]. This compound is an antibacterial and antimicrobial agent used in the treatment of both topical and internal infections. It can be found in

medications for vaginal and urinary tract infections as well as in medications for pneumonia, bowel diseases and other infections. It works by stopping the growth of yeast (fungus) that causes the infection. Further research may identify additional product or industrial usages of this chemical. Powdered sulfanilamide was used by the Allies in WWII to reduce infection rates.

In this work, we have studied the complexation of Sulfanilamide (SA) with three different crown ethers (CEs) (1) Dicyclohexano-18-crown-6 (DC18C6) [complex 1], (2) 18-crown-6 (18C6) [complex 2] and (3) Dibenzo-18-crown-6 (DB18C6) [complex 3] in acetonitrile (ACN). The complexes were characterized by ^{1}H NMR, IR and UV-visible spectra. The structure of the SA and all crown ethers are shown in **Scheme VII.1**.

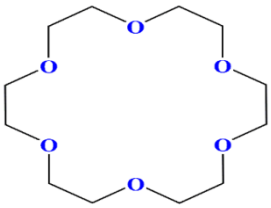

18-crown-6

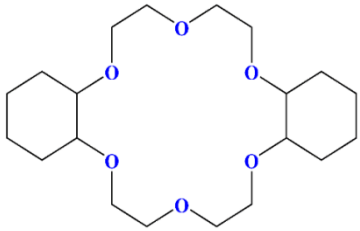

Dicyclohexano-18-crown-6

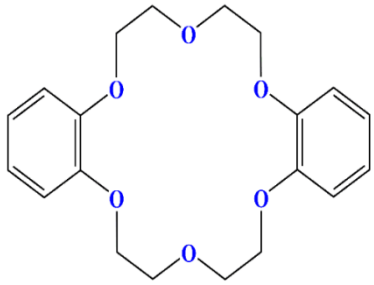

Dibenzo-18-crown-6

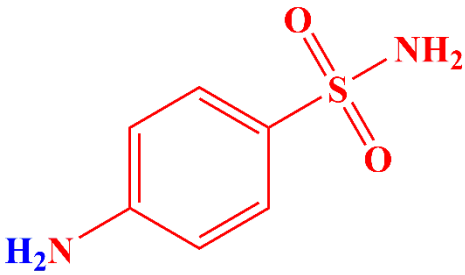

Sulphanilamide

Scheme VII.1: Molecular structure of crown ethers and SA.

VII.2. EXPERIMENTAL SECTION

VII.2.1 Reagents

The sulfa drug (99%) and crown ethers [18C6 (99%), DB18C6 (98%), DC18C6 (98%)] were bought from Sigma-Aldrich, Germany and used as purchased.

VII.2.2 Instrumentations

Prior to the start of the experimental work solubility of the chosen CEs and SA in ACN have been precisely checked and it was observed that the selected sulfa drug freely soluble in all proportion of CEs solution.

Infrared spectra were recorded in 8300 FT-IR spectrometer (Shimadzu, Japan). The details of the instrument have formerly been described [12]. The FTIR measurements were performed in the scanning range of 4000–400 cm^{-1} at room temperature.

^1H NMR spectra were recorded in CD_3CN at 300 MHz using Bruker ADVANCE 300 MHz instrument. Signals are quoted as δ values in ppm using residual protonated solvent signals as internal standard (CD_3CN: δ 1.97 ppm). Data are reported as chemical shift.

UV-visible spectra were recorded by JASCO V-530 UV/VIS Spectrophotometer, with an uncertainty of wavelength resolution of±2 nm. All the absorption spectra were recorded at 25°C ±1°C. The measuring temperature was held constant by an automated digital thermostat.

The densities (ρ) of the solutions were calculated by using vibrating *U*-tube Anton Paar digital density meter (DMA 4500M) having precision ±0.00005 g cm^{-3} and uncertainty in temperature was ±0.01K. The density meter was calibrated by standard method [13].

Viscosities (η) were determined by Brookfield DV-III Ultra Programmable Rheometer with spindle size 42. The detail has already been depicted before [13].

Refractive indexes of the solutions were studied with a Digital Refractometer from Mettler Toledo having uncertainty ±0.0002 units. The detail has already been described before [13].

VII.3. RESULT AND DISCUSSION

VII.3.1 Job plot demonstrate the Stoichiometry

The continuous variation method (Job's plot) was used to determine the stoichiometry of SA-CEs complexes [14, 15]. The plot of ΔA ×R against R represents the job plot where ΔA is the differences in absorbance of sulfa drug with and without CEs and R= [SA]/ [CEs] + [SA] and is presented in **Figure VII.1**. Absorbance values were measured at respective λ_{max} for a series of solutions at 298.15 K.

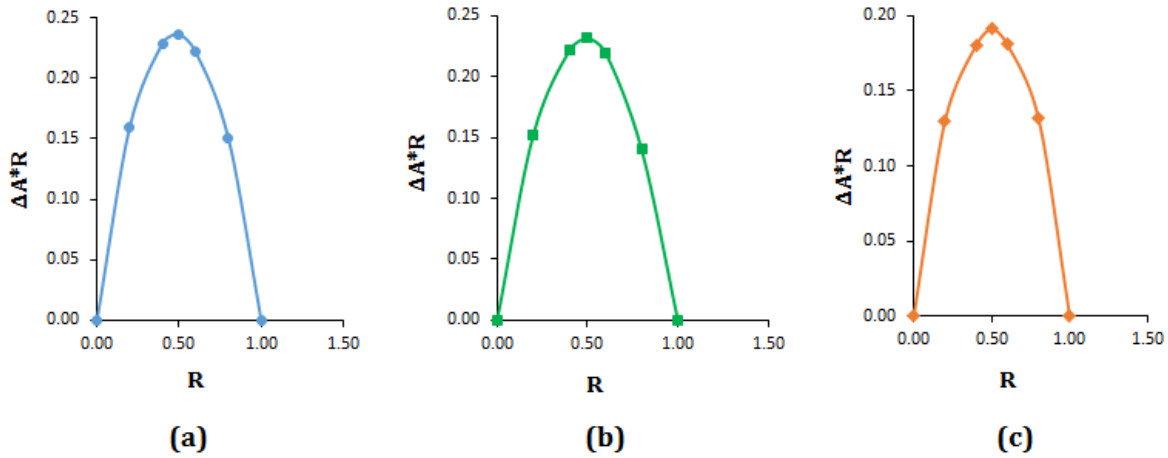

Figure VII.1: Job plot of (a) SA-DC18C6 system, (b) SA-18C6 system, (c) SA-DB18C6 system at T= 298.15 K.

In this method, the total molar concentration of the two binding partners ([SA] + [CEs]) is kept constant at 100μM but their mole fraction are varied so that the mole fractions of SA complete the range of 0-1 (**Table VII.1**, **Table VII.2** and **Table VII.3**) [16, 17].

Table VII.1: Data for the Job plot performed by UV-Vis spectroscopy for SA-DC18C6 system.

SA (mL)	DC18C6 (mL)	SA (μM)	DC18C6 (μM)	$R=\frac{[SA]}{[SA]+[DC18C6]}$	Absorbance (A)	ΔA	ΔA*R
0	3	0	100	0.0	0.0	1.01185	0.0
0.6	2.4	20	80	0.2	0.21129	0.80056	0.16011
1.2	1.8	40	60	0.4	0.43896	0.57289	0.22915
1.5	1.5	50	50	0.5	0.53905	0.47280	0.23640
1.8	1.2	60	40	0.6	0.64153	0.37032	0.22219
2.4	0.6	80	20	0.8	0.82361	0.18824	0.15059
3	0	100	0	1	1.01185	0.0	0.0

Table VII.2: Data for the Job plot performed by UV-Vis spectroscopy for SA-18C6 system.

SA (mL)	18C6 (mL)	SA (μM)	18C6 (μM)	$R=\frac{[SA]}{[SA]+[18C6]}$	Absorbance (A)	ΔA	ΔA*R
0	3	0	100	0.0	0.01981	0.99204	0.0
0.6	2.4	20	80	0.2	0.25067	0.76118	0.15224
1.2	1.8	40	60	0.4	0.45858	0.55327	0.22131
1.5	1.5	50	50	0.5	0.54919	0.46266	0.23133
1.8	1.2	60	40	0.6	0.64606	0.36579	0.21947
2.4	0.6	80	20	0.8	0.83681	0.17504	0.14003
3	0	100	0	1	1.01185	0.0	0.0

Table VII.3: Data for the Job plot performed by UV-Vis spectroscopy for SA-DB18C6 system.

SA (mL)	DB18C6 (mL)	SA (μM)	DB18C6 (μM)	$R=\frac{[SA]}{[SA]+[DB18C6]}$	Absorbance (A)	ΔA	ΔA*R
0	3	0	100	0.0	0.25859	0.75326	0.0
0.6	2.4	20	80	0.2	0.36268	0.64917	0.12983
1.2	1.8	40	60	0.4	0.56147	0.45038	0.18015
1.5	1.5	50	50	0.5	0.62905	0.38280	0.19140
1.8	1.2	60	40	0.6	0.72059	0.29126	0.17475
2.4	0.6	80	20	0.8	0.84731	0.16454	0.13163
3	0	100	0	1	1.01185	0.0	0.0

According to this method, maximum point of the molar ratio (R) corresponds to the complexation stoichiometry. The each of the three plots in **Figure VII.1** shows the maximum at a molar ratio of about 0.5, indicating that the complexes were formed with 1:1 stoichiometry.

VII.3.2 FTIR spectral analysis

The complexation between the sulfa drug (SA) and CEs was investigated using FTIR spectroscopy. **Figure VII.2**, **VII.3** and **VII.4** depict the FTIR spectra of free SA, 18C6, DC18C6, DB18C6 and their corresponding complexes in the 4000–500 cm^{-1} region. The investigation of the inclusion complexes was complicated due to the strong stretching frequency of CEs overlapping with the bands of the drugs. The IR spectrum of SA drug (**Figure VII.2**, **Figure VII.3** and **Figure VII.4**) was characterised by principal absorption peaks at 3382 and 3242 cm^{-1}(for NH stretching and antistretching in SO_2–NH group), 1310 cm^{-1}(for SO_2 asymmetric stretching), 1149 cm^{-1}(for SO_2 symmetric stretching) [18, 19]. The IR spectral features of the pure drug has changed in the complexes. The band assigned to the NH stretching and antistretching in SO_2–NH group were shifted in all the complexes (**Figure VII.2**, **VII.3** and **VII.4**). The symmetric and asymmetric vibrations of

SO_2 group at 1149 and 1310 cm^{-1} are shifted to 1124 cm^{-1} and 1290 cm^{-1} in complex 1, 1131 and 1296 cm^{-1} in complex 2 and 1130 and 1291 cm^{-1} in complex 3 respectively.

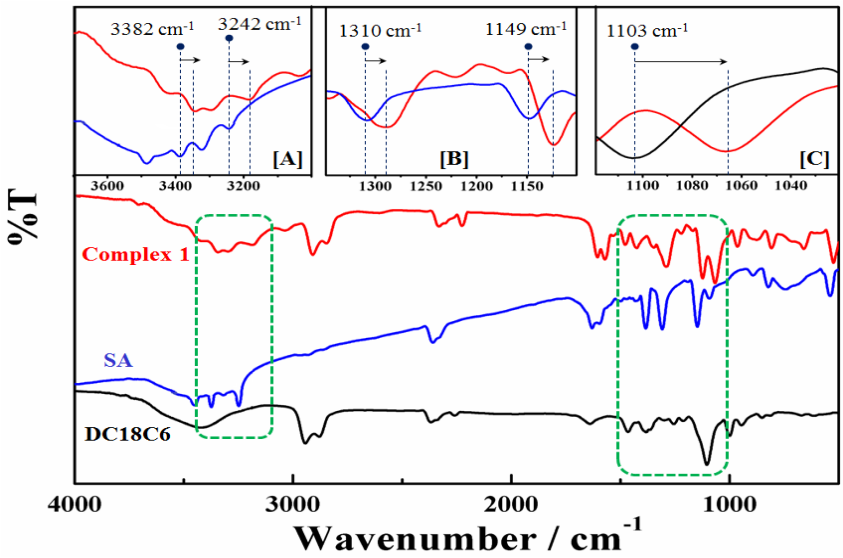

Figure VII.2: FTIR spectra of free DC18C6 (Black), SA (Blue) and complex 1 (Red).

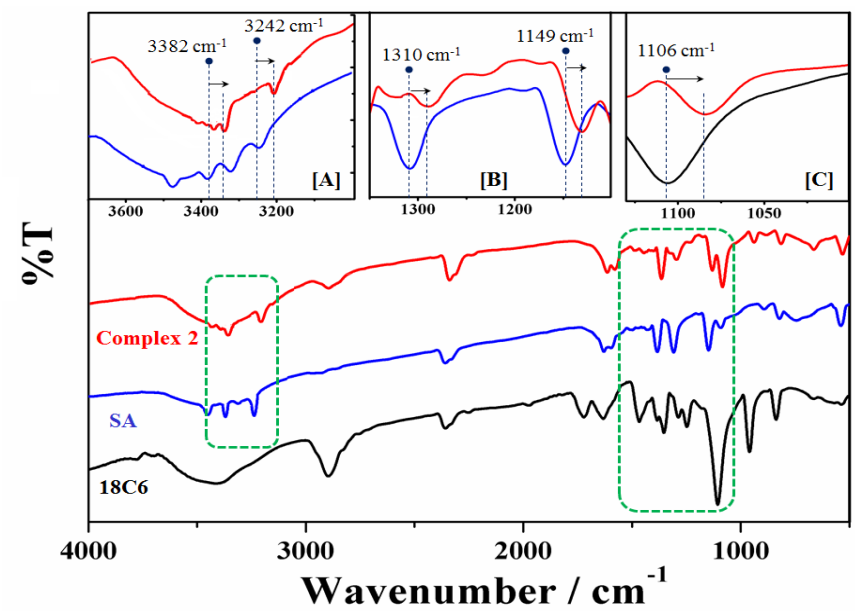

Figure VII.3: FTIR spectra of free 18C6 (Black), SA (Blue) and complex 2 (Red).

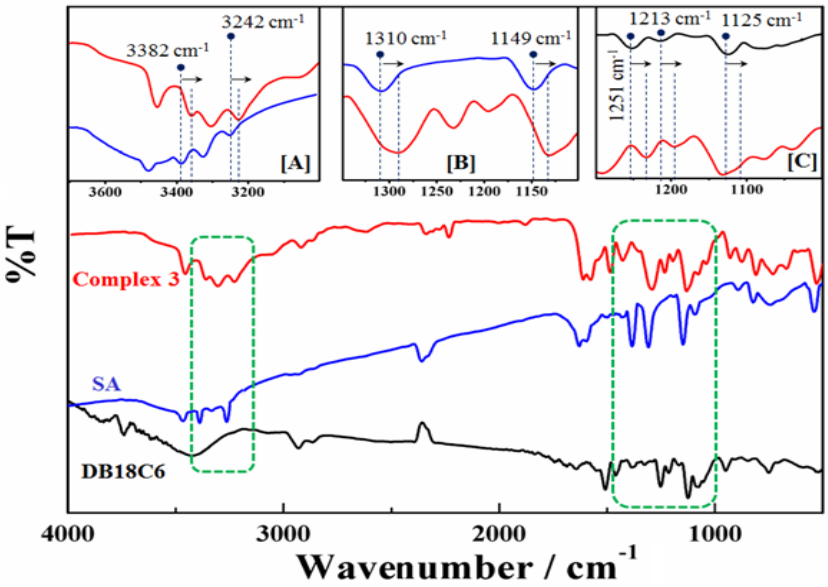

Figure VII.4: FTIR spectra of free DB18C6 (Black), SA (Blue) and complex 3 (Red).

In our investigation, the the NH stretching and anti-stretching in SO_2–NH group were shifted to 3346 and 3187 cm^{-1} in complex 1 (**Figure VII.2**), 3349 and 3203 cm^{-1} in complex 2 (**Figure VII.3**) and 3357 and 3220 in complex 3 (**Figure VII.4**). The above changes can be due to the formation of SA-CEs inclusion complex formation. According to the above FTIR analysis of all the three complexes, we might suggest that the sulfonamide ring of the SA was involved in the complexation. The bands positioned at 1103 cm^{-1} corresponding to the ν(C – O – C) of DC18C6 shifted to 1066 cm^{-1} in the complex 1 (**Figure VII.2**). The stretching frequencies of $\nu(C - O - C)_{aliph}$ of 18C6 at 1106 cm^{-1} shifted to 1083 cm^{-1} in the complex 2 (**Figure VII.3**). The shift of IR spectra of crown ethers in ACN solution indicates that the specific interactions observed in the crown ether complexes are in fact due to the hydrogen bonds of SA with the donor atoms of the crown ether. Comparing with the spectrum of the free crown ethers, most of these bands are shifted to lower energy presumably due to less restriction on the coupling of some vibrational modes caused by bonding of oxygen atoms of the polyether ring with the in both the complexes. The $\nu(C - O - C)_{arom}$ stretching vibrations of DB18C6 are observed at 1125 cm^{-1} and these peak is also shifted to lower frequency 1108 cm^{-1} in the complex

3 (**Figure VII.4**). The anisole oxygens of DB18C6 are also involved in H-bond formation in the complex 2, as indicated by the shifts of the ν_{as}(Ph-O-C) and ν_{s}(Ph-O-C) bands from 1213 and 1251 cm^{-1} to 1194 and 1231 cm^{-1}, respectively [20]. In the IR spectra, the bands in the 2800–3000 cm^{-1} region correspond to the CH stretching vibrations of the methylene groups of crown ethers. Selected IR data for the free compounds and their complexes and corresponding changes in frequencies are listed in **Table VII.4**.

Table VII.4: Comparison between the Frequencies change (cm^{-1}) of different functional group of free compound and their complexes.

Functional Group	Wavenumber (cm^{-1})		Changes (cm^{-1})
	DC18C6	**Complex 1**	**Δδ**
ν(C – O – C)	1103	1066	37
	18C6	**Complex 2**	
ν(C – O – C) aliph.	1106	1083	23
	DB18C6	**Complex 3**	
ν(C – O – C) arom	1125	1108	27
ν_{as}(Ph-O-C)	1213	1194	19
ν_{s}(Ph-O-C)	1251	1231	20
	SA	**Complex 1**	
$\nu_{as}(NH_2)_{sulfonamide}$	3382	3346	36
$\nu_{s}(NH_2)_{sulfonamide}$	3242	3187	55
$\nu_{as}(SO_2)$	1310	1290	20
$\nu_{s}(SO_2)$	1149	1124	25
	SA	**Complex 2**	
$\nu_{as}(NH_2)_{sulfonamide}$	3382	3349	33
$\nu_{s}(NH_2)_{sulfonamide}$	3242	3203	39
$\nu_{as}(SO_2)$	1310	1296	14
$\nu_{s}(SO_2)$	1149	1131	18
	SA	**Complex 3**	
$\nu_{as}(NH_2)_{sulfonamide}$	3382	3357	25
$\nu_{s}(NH_2)_{sulfonamide}$	3242	3220	22
$\nu_{as}(SO_2)$	1310	1291	19
$\nu_{s}(SO_2)$	1149	1130	19

VII.3.3 NMR Study

NMR spectroscopy has proved to be an efficient technique for the determination of the interactions between macrocyclic hosts and organic guests [21, 22]. A comparison of the ^{1}H NMR spectra revealed that the most significant change in the chemical shift of SA was observed in the move of the signal for $-NH_2$ protons (H2) of $-SO_2NH_2$ group towards higher field for complex 1 and complex 2 and lower field for complex 3 (**Figure VII.5-VII.7**) which suggests H-bonding via the protons of the sulfonyl group rather than amine group as the hydrogen atoms on the sulfonyl group are relatively acidic.

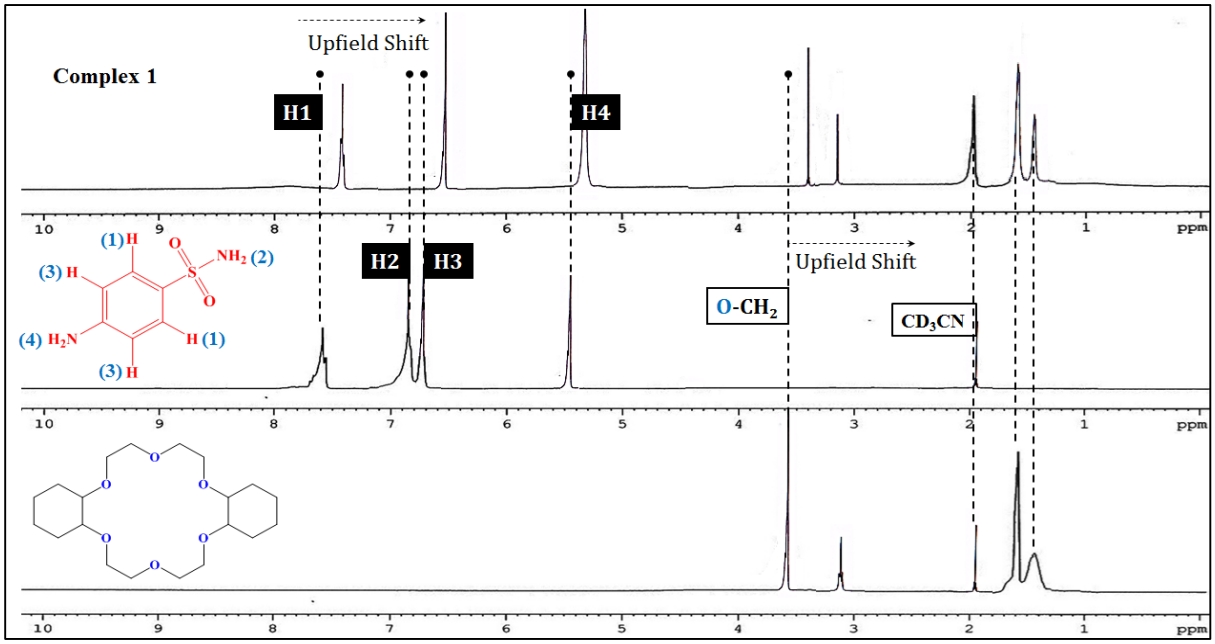

Figure VII.5: The ^{1}H NMR spectra of complex 1 (SA-DC18C6) (upper), uncomplexed SA and DC18C6 (lower) recorded at 300 MHz in CD_3CN at 298.15 K.

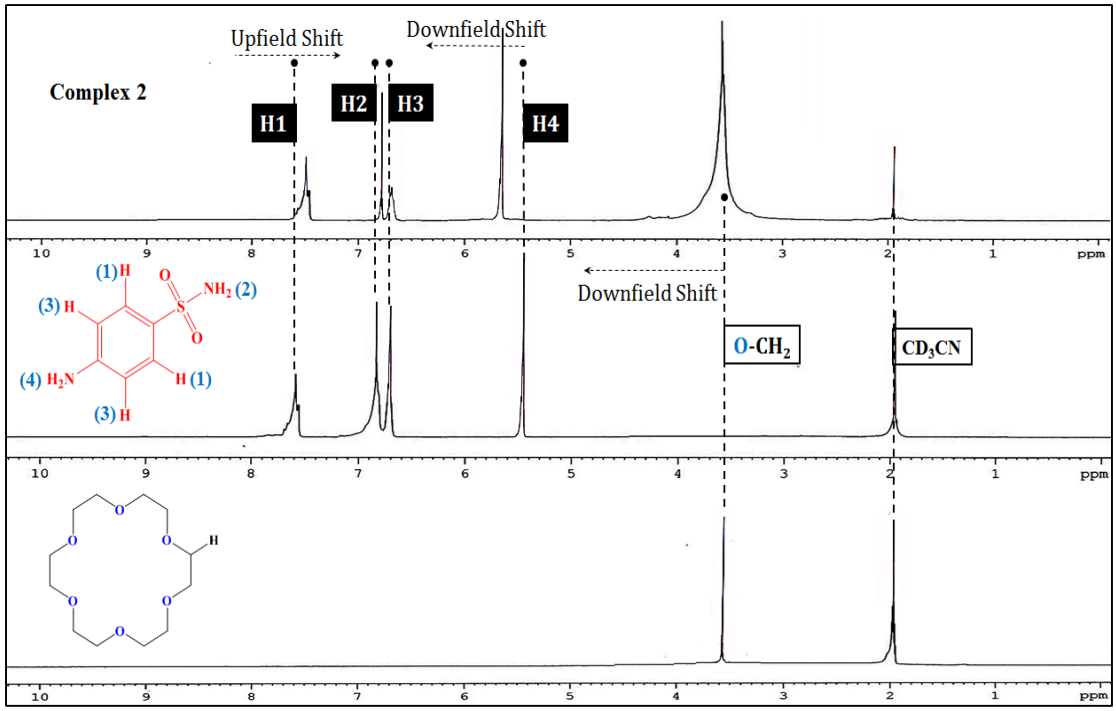

Figure VII.6: The ^{1}H NMR spectra of complex 2 (SA-18C6) (upper), uncomplexed SA and 18C6 (lower) recorded at 300 MHz in CD_3CN at 298.15 K.

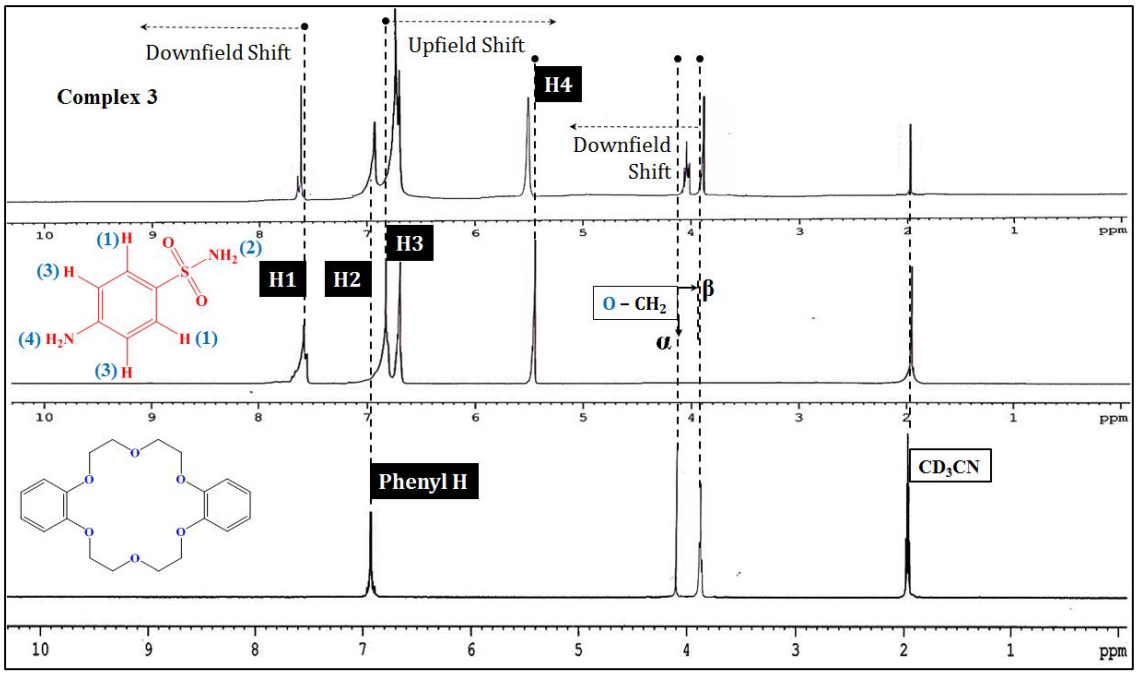

Figure VII.7: The ^{1}H NMR spectra of complex 3 (SA-DB18C6) (upper), uncomplexed SA and DB18C6 (lower) recorded at 300 MHz in CD_3CN at 298.15 K.

These changes in chemical shifts confirm the host-guest complexation of SA with all the studied crown ethers and gives the more accurate information about the conformations of host-guest complexes in solution which allows for a better understanding of molecular recognition [23-25]. Signals for the $-OCH_2$ protons of the crown ethers for complex 1 and complex 3 were found to be little upfield shifted relative to those signals for the free individual component (**Figure VII.5** and **Figure VII.7**). The observed upfield shift in **Figure VII.5** and **VII.7** represent, of course, the difference in the environment of the crown ether's $-OCH_2$ groups in the free and complexed ligand. In case of complex 2 $-OCH_2$ protons of the crown ether show downfield shift (**Figure VII.6**). The magnitude of the shift reflects the tightness of the crown-SA complex i.e., the overlap of the lone pair orbitals of the donating oxygen atoms of the macrocyclic ring and the outer orbitals of protons involved in H-bonding, which in turn induces a rather large change in the electronic environment of the $-OCH_2$ groups.

Selected ^{1}H NMR data

Sulfanilamide (SA): ^{1}H NMR (CD_3CN, 298.15 K): δ 7.56-7.71 (aryl, 2H), 6.81-6.84 ($-SO_2NH_2$, 2H), 6.69-6.72 (aryl, 2H), 5.47-5.51(aniline $-NH_2$, 2H).

18-crown-6(18C6): ^{1}H NMR (CD_3CN, 298.15 K): δ 3.52-3.59 (OCH_2, 24H).

Dicyclohexano-18-crown-6(DC18C6): ^{1}H NMR (CD_3CN, 298.15 K): δ 3.54-3.59 (OCH_2, 16H), 3.11-3.13(cyclohexane, 4H), 1.56-1.59 (cyclohexane, 8H), 1.39-1.50 (cyclohexane, 8H).

Dibenzo-18-crown-6(DB18C6): ^{1}H NMR (CD_3CN, 298.15 K): δ 6.89-6.96 (aryl, 8H), 4.10-4.13 (OCH_2, 8H), 3.85-3.88 (OCH_2, 8H).

DC18C6-SA (complex 1): ^{1}H NMR (CD_3CN, 298.15 K): δ 7.37-7.46 (aryl, 2H), 6.55-6.59 ($-SO_2NH_2$, 2H), 6.49-6.52 (aryl, 2H), 5.34-5.41 (aniline $-NH_2$, 2H), 3.34-3.38 (OCH_2, 16H).

18C6-SA (complex 1): ^{1}H NMR (CD_3CN, 298.15 K): δ 7.55-7.66 (aryl, 2H), 6.79-6.80 ($-SO_2NH_2$, 2H), 6.68-6.72 (aryl, 2H), 5.62-5.63 (aniline $-NH_2$, 2H), 3.46-3.69 (m, OCH_2, 24H).

DB18C6-SA (complex 3): ^{1}H NMR (CD_3CN, 298.15 K): δ 7.57-7.79 (aryl, 2H), 6.90-6.95 ($-SO_2NH_2$, 2H), 5.48-5.49 (aniline $-NH_2$, 2H), 6.90-6.95 (aryl, 8H), 4.03-4.12 (OCH_2, 8H), 3.83-3.85 (OCH_2, 8H).

VII.3.4 Apparent molar volume

The interactions between SA and cyclic CEs can be studied from the apparent molar volume (ϕ_V) and limiting apparent molar volume (ϕ_V^0) [26]. The apparent molar volume can be considered to be the sum of the geometric volume of the solute molecule and changes in the solvent volume due to its interaction with the solute [27]. For this purpose, the apparent molar volumes ϕ_V were determined from the solutions densities (**Table VII.5**) using the following equation

$$\phi_V = M/\rho - (\rho - \rho_o)/m\rho_o\rho \qquad (1)$$

where M is the molar mass of the solute, m is the molality of the solution, ρ and ρ_0 are the densities of the solution and reference solvent [crown ether + ACN], respectively.

Table VII.5: Experimental values of density (ρ) and viscosity (η) of sulfa drug in different mass fraction of DC18C6 (w_1), 18C6 (w_2) and DB18C6 (w_3) in ACN at T= (293.15 to 308.15) K.

m **/mol kg^{-1}**	**$\rho\cdot10^{-3}$ /kg·m^{-3}**	**η /mPa·s**	**$\rho\cdot10^{-3}$ /kg·m^{-3}**	***H*** **/mPa·s**	**$\rho\cdot10^{-3}$ /kg·m^{-3}**	**η /mPa·s**	**$\rho\cdot10^{-3}$ /kg·m^{-3}**	**η /mPa·s**
Sulfa+DC186								
w_1=0.001[b]								
	293.15 K[a]		298.15 K[a]		303.5 K[a]		308.15 K[a]	
0.001	0.78249	0.38	0.77710	0.37	0.77165	0.36	0.76619	0.35
0.003	0.78263	0.38	0.77724	0.37	0.77179	0.36	0.76633	0.35
0.005	0.78277	0.38	0.77738	0.38	0.77193	0.36	0.76647	0.35
0.007	0.78292	0.39	0.77753	0.38	0.77208	0.36	0.76661	0.36
0.009	0.78308	0.39	0.77768	0.39	0.77223	0.37	0.76676	0.36
w_1=0.003[b]								
0.001	0.78290	0.40	0.77753	0.39	0.77209	0.37	0.76663	0.36
0.003	0.78302	0.40	0.77765	0.39	0.77221	0.37	0.76675	0.36
0.005	0.78316	0.40	0.77778	0.39	0.77234	0.38	0.76688	0.36
0.007	0.78329	0.41	0.77792	0.40	0.77248	0.38	0.76702	0.37
0.009	0.78344	0.41	0.77806	0.40	0.77262	0.38	0.76716	0.37

				w_1=0.005^b				
0.001	0.78316	0.42	0.77777	0.41	0.77236	0.38	0.76690	0.36
0.003	0.78327	0.42	0.77788	0.41	0.77247	0.38	0.76701	0.36
0.005	0.78339	0.43	0.77800	0.41	0.77258	0.39	0.76712	0.37
0.007	0.78351	0.43	0.77812	0.42	0.77270	0.39	0.76724	0.37
0.009	0.78364	0.43	0.77824	0.42	0.77283	0.39	0.76736	0.37
				Sulfa+18C6				
				w_2=0.001^b				
0.001	0.78241	0.37	0.77702	0.36	0.77161	0.35	0.76615	0.34
0.003	0.78257	0.37	0.77718	0.36	0.77176	0.35	0.76630	0.34
0.005	0.78273	0.37	0.77734	0.37	0.77192	0.35	0.76645	0.34
0.007	0.78290	0.38	0.77750	0.37	0.77208	0.36	0.76661	0.35
0.009	0.78307	0.38	0.77767	0.37	0.77224	0.36	0.76677	0.35
				w_2=0.003^b				
0.001	0.78283	0.37	0.77745	0.37	0.77201	0.36	0.76655	0.35
0.003	0.78296	0.38	0.77758	0.37	0.77215	0.36	0.76669	0.35
0.005	0.78311	0.38	0.77773	0.37	0.77229	0.36	0.76683	0.35
0.007	0.78326	0.38	0.77787	0.38	0.77243	0.37	0.76697	0.36
0.009	0.78341	0.38	0.77803	0.38	0.77258	0.37	0.76712	0.36
				w_2=0.005^b				
0.001	0.78311	0.40	0.77772	0.38	0.77230	0.36	0.76684	0.35
0.003	0.78323	0.40	0.77784	0.38	0.77242	0.37	0.76696	0.35
0.005	0.78336	0.40	0.77797	0.38	0.77255	0.37	0.76709	0.35
0.007	0.78350	0.41	0.77811	0.39	0.77268	0.37	0.76722	0.35
0.009	0.78364	0.41	0.77825	0.39	0.77282	0.38	0.76736	0.36
				Sulfa+DB186				
				w_3=0.001^b				
0.001	0.78237	0.34	0.77698	0.32	0.77157	0.31	0.76609	0.29
0.003	0.78252	0.35	0.77713	0.33	0.77173	0.32	0.76625	0.30
0.005	0.78268	0.35	0.77729	0.33	0.77188	0.32	0.76640	0.30
0.007	0.78284	0.35	0.77745	0.33	0.77204	0.32	0.76656	0.30
0.009	0.78301	0.35	0.77761	0.33	0.77220	0.32	0.76672	0.31

w_3=0.003[b]								
0.001	0.78269	0.36	0.77730	0.35	0.77189	0.32	0.76643	0.32
0.003	0.78282	0.36	0.77743	0.35	0.77202	0.33	0.76656	0.32
0.005	0.78296	0.36	0.77757	0.35	0.77215	0.33	0.76669	0.32
0.007	0.78310	0.37	0.77771	0.36	0.77229	0.33	0.76683	0.33
0.009	0.78325	0.37	0.77785	0.36	0.77243	0.34	0.76697	0.33
w_3=0.005[b]								
0.001	0.78292	0.37	0.77753	0.35	0.77211	0.32	0.76664	0.32
0.003	0.78304	0.37	0.77765	0.35	0.77223	0.33	0.76676	0.32
0.005	0.78317	0.37	0.77778	0.35	0.77236	0.33	0.76689	0.32
0.007	0.78330	0.38	0.77791	0.36	0.77249	0.33	0.76701	0.33
0.009	0.78344	0.38	0.77804	0.36	0.77262	0.33	0.76714	0.33

[a]Standard uncertainties in temperature (T) = ±0.01 K.

[b]w_1, w_2 and w_2 are the mass fraction of the solvent (ACN+DC18C6), (ACN+18C6), (ACN+DB18C6) respectively.

The values of ϕ_V are large and positive for all the systems, suggesting strong solute-solvent interactions. The values of the the apparent molar volume at infinite dilution (ϕ_V^0) and the experimental slopes (S_V^*) were determined by using least squares fitting of the linear plots of ϕ_V against the square root of the molar concentrations ($m^{1/2}$) in accordance with the Masson equation [28].

$$\phi_V = \phi_V^0 + S_V^* \cdot \sqrt{m} \qquad (2)$$

The calculated values of ϕ_V^0 and S_V^* are reported in **Table VII.6**. This table shows that positive values of ϕ_V^0 for all the three complexes increases with an increase in mass fraction of the respective crown and temperature (**Figure VII.8**) which indicates that stronger interaction occur between SA and CEs in ACN solvent at higher mass fraction of crown ether and high temperature [29, 30]. Since S_V^* values for large organic molecules are not of much significance, they have not been discussed here [31]. The observed ϕ_V^0 positive values (**Table VII.6**) are mainly due to the interactions between acidic protons

of $-SO_2NH_2$ group and lone pair of electrons of O_{crown}. From **Figure VII.6** it can be observed that ϕ_V^0 values for SA in complex 1 is highest, then complex 1 and then complex 3. This can be explained on the basis of the strength of the interacting groups present in the crown ethers molecules. In complex 1 i.e. complex of DC18C6, electron pumping of cyclohexyl groups of DC18C6 is a major reason that its complex is more stable than those with 18C6, most possibly due to the increased basicity of the oxygen atoms of the ring, as H-bond acceptors. In the case of complex 3 i.e complex of DB18C6, the electron-withdrawing power of the benzo group(s) which weaken the electron-donor ability of the oxygen atoms resulting in a weaker interaction. Thus from this study, we can say that the trend in the solute-solvent interaction is

Complex 3 < complex 2< complex 1

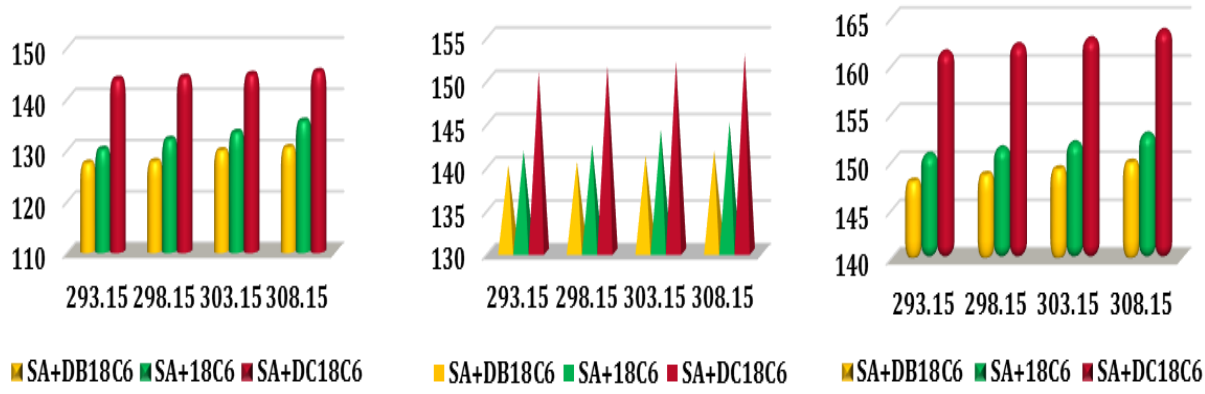

(a) **(b)** **(c)**

Figure VII.8: Plot of limiting apparent molar volume (ϕ_V^0) of SA in mass fractions (a) 0.001, (b) 0.003, (c) 0.005 (w) of different CEs in ACN at T= (293.15 to 308.15)K respectively.

Table VII.6: Limiting apparent molar volume (ϕ_V^0) and viscosity *B*-coefficient of sulfa drug in different mass fraction of different crown ethers in ACN at T= (293.15 to 308.15) K.

Temp/K[a]	$\phi_V^0 \cdot 10^6$ /m³·mol⁻¹	$S_V^* \cdot 10^6$ /m³·mol⁻³/²·kg¹/²	*B* /kg¹/²·mol⁻¹/²
SA+DC18C6		**w_1 = 0.001[b]**	
293.15	143.75±0.01	-146.86	0.5357±0.0080
298.15	144.16±0.00	-135.29	0.5475±0.0147
303.15	144.71±0.01	-126.16	0.5556±0.0219
308.15	145.29±0.01	-112.42	0.5674±0.0259
SA+18C6		**w_2 = 0.001[b]**	
293.15	130.12±0.01	-129.53	0.3639±0.0257
298.15	132.04±0.01	-119.47	0.4090±0.0297
303.15	133.42±0.02	-102.75	0.4281±0.0219
308.15	135.62±0.00	-97.90	0.4631±0.0271
SA+DB18C6		**w_3 = 0.001[b]**	
293.15	127.43±0.01	-86.41	0.2948±0.0380
298.15	127.73±0.01	-74.63	0.3648±0.0268
303.15	129.85±0.01	-70.02	0.3859±0.0174
308.15	130.47±0.01	-63.48	0.4597±0.0133
SA+DC18C6		**w_1 = 0.003[b]**	
293.15	151.05±0.01	-149.01	0.6482±0.0165
298.15	151.97±0.01	-139.49	0.6553±0.0266
303.15	152.66±0.00	-131.80	0.6745±0.0157
308.15	153.73±0.02	-126.72	0.6912±0.0254
SA+18C6		**w_2 = 0.003[b]**	
293.15	141.72±0.01	-137.14	0.4951±0.0049
298.15	142.43±0.01	-123.67	0.5506±0.0080
303.15	144.17±0.01	-108.21	0.6054±0.0167
308.15	144.97±0.01	-103.23	0.6904±0.0126

SA+DB18C6		**w_3 = 0.003[b]**	
293.15	140.05±0.01	-88.73	0.3930±0.0211
298.15	140.46±0.01	-73.19	0.4437±0.0098
303.15	141.10±0.02	-58.04	0.5221±0.0160
308.15	141.72±0.01	-50.03	0.6012±0.0170
SA+DC18C6		**w_1 = 0.005[b]**	
293.15	161.51±0.01	-155.69	0.7414±0.0157
298.15	162.28±0.00	-144.31	0.7930±0.0000
303.15	162.88±0.01	-133.79	0.8243±0.0290
308.15	163.73±0.01	-124.02	0.8704±0.0290
SA+18C6		**w_2 = 0.005[b]**	
293.15	150.87±0.01	-137.59	0.5921±0.0117
298.15	151.53±0.01	-129.91	0.6407±0.0181
303.15	152.06±0.00	-115.89	0.6810±0.0150
308.15	152.97±0.01	-108.57	0.7268±0.0123
SA+DB18C6		**w_3 = 0.005[b]**	
293.15	148.03±0.01	-95.43	0.4796±0.0204
298.15	148.72±0.01	-85.25	0.5399±0.0080
303.15	149.31±0.01	-72.50	0.6141±0.0106
308.15	149.99±0.01	-61.08	0.6977±0.0202

[a]Standard uncertainties in temperature (T) = ±0.01 K.

[b]w_1, w_2 and w_2 are the mass fraction of the solvent (ACN+DC18C6), (ACN+18C6), (ACN+DB18C6) respectively.

VII.3.5 Temperature dependent limiting apparent molar volume

The temperature dependence of ϕ_V^0 values can be expressed by the general polynomial equation as follows,

$$\phi_V^0 = a_0 + a_1 T + a_2 T^2 \qquad (3)$$

where a_0, a_1, a_2 are the empirical coefficients and the values of these coefficients have been evaluated by the least-squares fitting of apparent molar volume at different temperatures [**Table VII.7**].

Table VII.7: Values of empirical coefficients (a_0, a_1, and a_2) of Equation 14 of sulfa drug in different mass fraction of DC18C6 (w_1), 18C6 (w_2) and DB18C6 (w_3) in ACN at T= (293.15 to 308.15) K.

Mass fraction	$a_0 \cdot 10^6$ /$m^3 \cdot mol^{-1}$	$a_1 \cdot 10^6$ /$m^3 \cdot mol^{-1} \cdot K^{-1}$	$a_2 \cdot 10^6$ /$m^3 \cdot mol^{-1} \cdot K^{-2}$
SA + DC18C6			
w_1 = 0.001[b]	267.00	-0.919	0.0017
w_1 = 0.003[b]	235.40	-0.727	0.0015
w_1 = 0.005[b]	191.23	-0.336	0.0008
SA + 18C6			
w_1 = 0.001[b]	278.29	-1.326	0.0028
w_1 = 0.003[b]	155.56	-0.311	0.0009
w_1 = 0.005[b]	336.69	-1.367	0.0025
SA + DB18C6			
w_1 = 0.001[b]	350.43	-1.699	0.0032
w_1 = 0.003[b]	296.61	-1.150	0.0021
w_1 = 0.005[b]	171.94	-0.287	0.0007

[b] w_1, w_2 and w_2 are the mass fraction of the solvent (ACN+DC18C6), (ACN+18C6), (ACN+DB18C6) respectively.

The limiting apparent molar expansibilities, ϕ_E^0, can be obtained by the following equation,

$$\phi_E^0 = \left(\delta\phi_V^0/\delta T\right)_P = a_1 + 2a_2T \qquad (4)$$

Differentiation of eq. 4 with respect to temperature gives the values of the limiting apparent molar expansibilities (ϕ_E^0) [**Table VII.8**]. These values are also employed in

interpreting of the structure-making or breaking properties of various solutes. Positive expansivity i.e increasing volume with increasing temperature is a characteristic property of nonaqueous solutions of hydrophobic solvation [32].

Table VII.8: Limiting apparent molal expansibilities (ϕ_E^0) of sulfa drug in different mass fraction of DC18C6 (w_1), 18C6 (w_2) and DB18C6 (w_3) in ACN at T= (293.15 to 308.15) K.

Mass fraction	$\phi_E^0 \cdot 10^6$ **/m³·mol⁻¹·K⁻¹**				$\left(\partial\phi_E^0/\partial T\right)_P \cdot 10^6$ **/m³·mol⁻¹·K⁻²**
			SA + DC18C6		
T/K[a]	293.15	298.15	303.15	308.15	
w_1 = 0.001[b]	0.078	0.095	0.112	0.129	0.003
w_1 = 0.003[b]	0.152	0.167	0.182	0.197	0.003
w_1 = 0.005[b]	0.133	0.141	0.149	0.157	0.002
			SA + 18C6		
T/K[a]	293.15	298.15	303.15	308.15	
w_2 = 0.001[b]	0.316	0.344	0.372	0.400	0.006
w_2= 0.003[b]	0.216	0.225	0.234	0.243	0.002
w_2= 0.005[b]	0.099	0.124	0.149	0.174	0.005
			SA + DB18C6		
T/K[a]	293.15	298.15	303.15	308.15	
w_3 = 0.001[b]	0.177	0.209	0.241	0.273	0.006
w_3= 0.003[b]	0.081	0.103	0.124	0.145	0.004
w_3 = 0.005[b]	0.124	0.131	0.138	0.145	0.001

[a]Standard uncertainties in temperature (T) = ±0.01 K.

[b]w_1, w_2 and w_2 are the mass fraction of the solvent (ACN+DC18C6), (ACN+18C6), (ACN+DB18C6) respectively.

Hepler [33] developed a technique of examining the sign of $\left(\delta\phi_E^0/\delta T\right)_P$ for the solute in terms of long-range structure-making and -breaking capacity of the solute in the solution using the general thermodynamic expression,

$$\left(\delta\phi_E^0/\delta T\right)_P = \left(\delta^2\,\phi_V^0/\delta T^2\right)_P = 2a_2 \qquad (5)$$

If the sign of the second derivatives of the limiting apparent molar volume with respect to the temperature $\left(\delta\phi_E^0/\delta T\right)_P$ is positive or a small negative, the molecule is a structure maker; otherwise, it is a structure breaker [34]. As is evident from **Table VII.8**, the $\left(\delta\phi_E^0/\delta T\right)_P$ values for all the complexes are positive i.e. SA is predominantly structure makers in all of the complexes of crown ethers and this tendency is enhanced with increasing crown concentration.

VII.3.6 Viscosity B Coefficients

The experimental viscosity (η) data measured at different temperatures for the studied systems are tabulated in **Table VII.5**. The relative viscosity (η_r) has been analyzed using the Jones-Dole equation [35]

$$(\eta/\eta_o - 1)/\sqrt{m} = (\eta_r - 1)/\sqrt{m} = A + B\sqrt{m} \qquad (6)$$

Where relative viscosity $\eta_r = \eta/\eta_o$, η and η_0 are the viscosities of the ternary solutions (SA + crown ether + ACN) and binary reference solvent (crown ether + ACN), respectively, and *m* is the molality of the SA in the ternary solutions. *A* and *B* are experimental constants known as viscosity *A*- and *B*-coefficients, which are specific to solute-solute and solute-solvent interactions, respectively. The values of *B* coefficients are obtained from the slope of linear plot of $(\eta_r - 1)/\sqrt{m}$ against $\sqrt{m}$ by least-squares method, and reported in **Table VII.6**.

B-Coefficients are known to provide information regarding the solvation of the solutes and their effects on the structure of the solvent in the near environment of the solute molecules [36,37]. The values of B-coefficient for SA in complex 1 are highest of the three complexes and the smallest for complex 3 in ACN [**Table VII.6**]. Positive values of the B-coefficient suggest hydrogen bonding of the solvent with the drug molecule and

indicate an increase in viscosity of the solution due to the large size of the moving molecules. The solvated solutes molecule associated by the solvent molecules all round to the formation of associated molecule by solute-solvent interaction are responsible for the higher values of the *B*-coefficient, would present greater resistance, and this type of interactions are strengthened with a rise in temperature and also increase with an increase of mass fraction of CEs in the solvent mixtures [**Figure VII.9**].

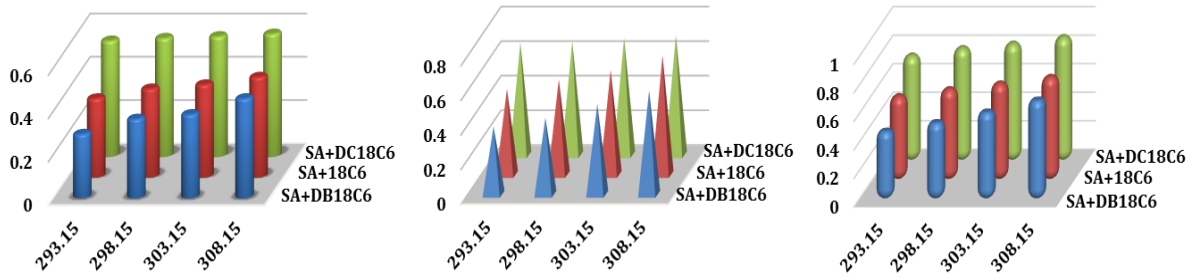

(a) **(b)** **(c)**

Figure VII.9: Plot of viscosity B-coefficient of SA in mass fractions (a) 0.001, (b) 0.003, (c) 0.005 (w) of different CEs in ACN at T= (293.15 to 308.15)K respectively.

These observations are in excellent agreement with the conclusions drawn from the analysis of apparent molar volume, ϕ_V^0 discussed earlier. The calculated values of dB/dT are small positive shown in **Table VII.9** reflects the structure-maker behaviors of the sulfa drug [27].

Table VII.9: Values of *dB/dT* of sulfa drug in different mass fraction of DC18C6 (w_1), 18C6 (w_2) and DB18C6 (w_3) in ACN at T= (293.15 to 308.15) K respectively.

Mass fraction	$\frac{dB}{dT}$ /kg$^{1/2}$·mol$^{1/2}$·K^{-1}				
	SA + DC18C6		SA + 18C6		SA + DB18C6
w_1 = 0.001[b]	0.006	w_2 = 0.001[b]	0.002	w_3 = 0.001[b]	0.010
w_1 = 0.003[b]	0.012	w_2= 0.003[b]	0.003	w_3= 0.003[b]	0.014
w_1 = 0.005[b]	0.008	w_2= 0.005[b]	0.008	w_3 = 0.005[b]	0.014

[b]w_1, w_2 and w_2 are the mass fraction of the solvent (ACN+DC18C6), (ACN+18C6), (ACN+DB18C6) respectively.

Thus, the volumetric and viscometric properties of the sulfa drug in the present work provide useful information in medicinal and pharmaceutical chemistry for the prediction of absorption and permeability of drug through membranes.

VII.3.7 Refractive index calculation

Experimental refractive index data n_D for (SA + crown ether + ACN) ternary solutions were measured as a function of the molarities of several crown ethers at T =298.15 K. The values of measured n_D are tabulated in **Table VII.10**. The molar refraction R_M can be evaluated from the Lorentz-Lorenz relation [38].

$$R_M = \left\{(n_D^2\text{-}1)/(n_D^2+2)\right\}(M/\rho) \quad (7)$$

Where R_M, n_D, M and ρ are the molar refraction, the refractive index, the molar mass and the density of solution respectively. Because the R_M value is directly proportional to molecular polarizability [39], this quantity is a measure of the ability of the molecular orbitals to be impaired under an electrical field [40].

Table VII.10 indicates that the R_M values increase with an increasing amount of crown in the ternary solutions studied because its electron cloud becomes more decentralized, indicating high polarizability in the presence of crown ethers. The

refractive index, molar refraction (R_M) and consequently the limiting molar refraction (R_M^0) (**Table VII.11**) values of a substance is higher when its molecules are more tightly packed or in general when the compound is denser. In the present ternary solution system, the interactions occurring between the SA and three different crown ether are explored. It is evident from **Figure VII.10** that DC18C6 interacts more strongly with SA than with 18C6 and DB18C6 which is probably due to stable complex formation of DC18C6 through the H-bond formation between acidic protons of sulfonyl group (-SO_2NH_2) and O_{crown} i.e. DC18C6 form compact structure which is reflected in their high R_M^0 values; moreover, the strength of the interactions are increases with increasing molarity of crown.

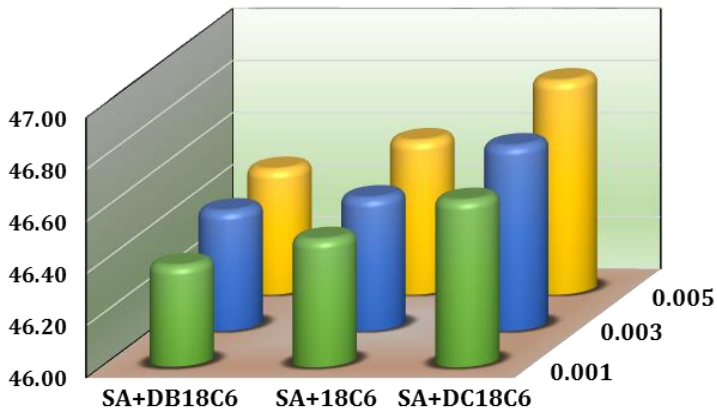

Figure VII.10: Plot of limiting molar refraction (R_M^o) of SA in different mass fractions (w) of different CEs in ACN at T= 298.15 K respectively.

Table VII.10: Values of Refractive Index (n_D) and Molar Refraction (R_M) of sulfa drug in different mass fraction of DC18C6 (w_1), 18C6 (w_2) and DB18C6 (w_3) in ACN at T= 298.15 K respectively.

	Conc. (m)	n_D	R_M **/m³·mol⁻¹**
***w₁* = 0.001[b]**			
SA + DC18C6	0.001	1.3428	46.79
	0.003	1.3436	46.88
	0.005	1.3442	46.95
	0.007	1.3447	47.00
	0.009	1.3452	47.06
***w₂* = 0.001[b]**			
SA + 18C6	0.001	1.3415	46.64
	0.003	1.3422	46.72
	0.005	1.3429	46.79
	0.007	1.3435	46.86
	0.009	1.3440	46.91
***w₃* = 0.001[b]**			
SA + DB18C6	0.001	1.3409	46.57
	0.003	1.3417	46.66
	0.005	1.3423	46.72
	0.007	1.3429	46.79
	0.009	1.3435	46.85
w_1 = 0.003[b]			
SA + DC18C6	0.001	1.3436	46.87
	0.003	1.3443	46.95
	0.005	1.3449	47.01
	0.007	1.3454	47.07
	0.009	1.3459	47.12

w_2= 0.003[b]			
SA + 18C6	0.001	1.3423	46.71
	0.003	1.3431	46.80
	0.005	1.3438	46.88
	0.007	1.3445	46.96
	0.009	1.3451	47.02
w_3= 0.003[b]			
SA + DB18C6	0.001	1.3416	46.63
	0.003	1.3423	46.71
	0.005	1.3429	46.78
	0.007	1.3436	46.86
	0.009	1.3440	46.90
w_1 = 0.005[b]			
SA + DC18C6	0.001	1.3450	47.03
	0.003	1.3459	47.13
	0.005	1.3465	47.21
	0.007	1.3473	47.29
	0.009	1.3479	47.35
w_2= 0.005[b]			
SA + 18C6	0.001	1.3428	46.76
	0.003	1.3436	46.85
	0.005	1.3442	46.91
	0.007	1.3448	46.98
	0.009	1.3453	47.03
w_3 = 0.005[b]			
SA + DB18C6	0.001	1.3421	46.68
	0.003	1.3430	46.79
	0.005	1.3437	46.86
	0.007	1.3444	46.94
	0.009	1.3450	47.01

[b]w_1, w_2 and w_2 are the mass fraction of the solvent (ACN+DC18C6), (ACN+18C6), (ACN+DB18C6) respectively.

Table VII.11: Limiting molar refractions (R_M^0) values of sulfa drug in different mass fraction of DC18C6 (w_1), 18C6 (w_2) and DB18C6 (w_3) in ACN at T= 298.15 K respectively.

Mass fraction	R_M^0 /m^3·mol^{-1}		
	SA + DC18C6	SA + 18C6	SA + DB18C6
w_1 = 0.001[b]	46.64	46.49	46.64
w_1 = 0.003[b]	46.71	46.51	46.71
w_1 = 0.005[b]	46.82	46.59	46.82

[b]w_1, w_2 and w_2 are the mass fraction of the solvent (ACN+DC18C6), (ACN+18C6), (ACN+DB18C6) respectively.

VII.3.8 Typical Features of Specific Interactions involved in the Complexation

The all three complexes of CEs (**Scheme VII.2**) are stabilized mainly by hydrogen bonds formed between acidic protons of –NH_2 group and ether oxygen atoms. This can be shown by the suitable plausible mechanism (**Scheme VII.2**).But in case of complex 3 i.e. complex of DB18C6, hydrogen bonding seems to play a secondary role because the benzene rings of the DB18C6 decrease the negative charge of the oxygen atoms and hence their ability to undergo hydrogen bonding. The π–π interaction is present only in this complex which also slightly stabilized the complex (**Scheme VII.2**) [41-43].

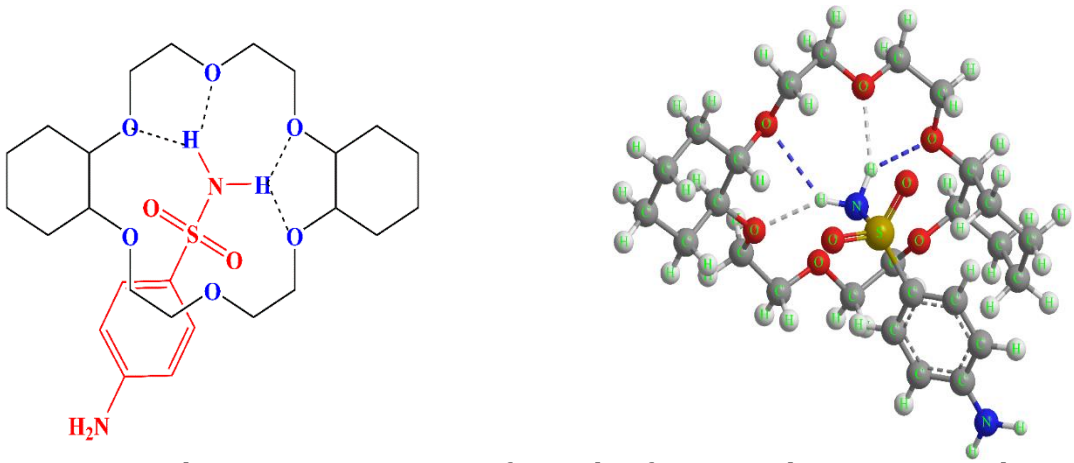

Scheme VII.2a: Schematic presentation of complex formation between SA and DC18C6 and corresponding energy minimized structure of the complex.

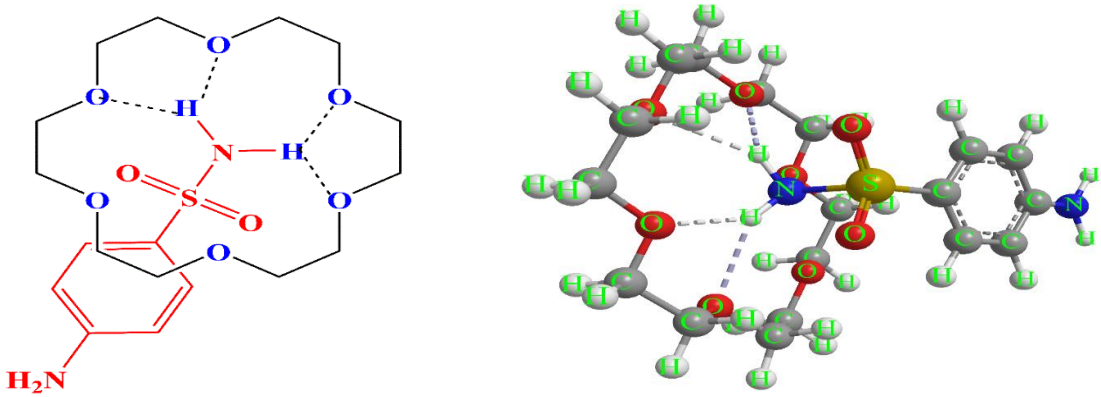

Scheme VII.2b: Schematic presentation of complex formation between SA and 18C6 and corresponding energy minimized structure of the complex.

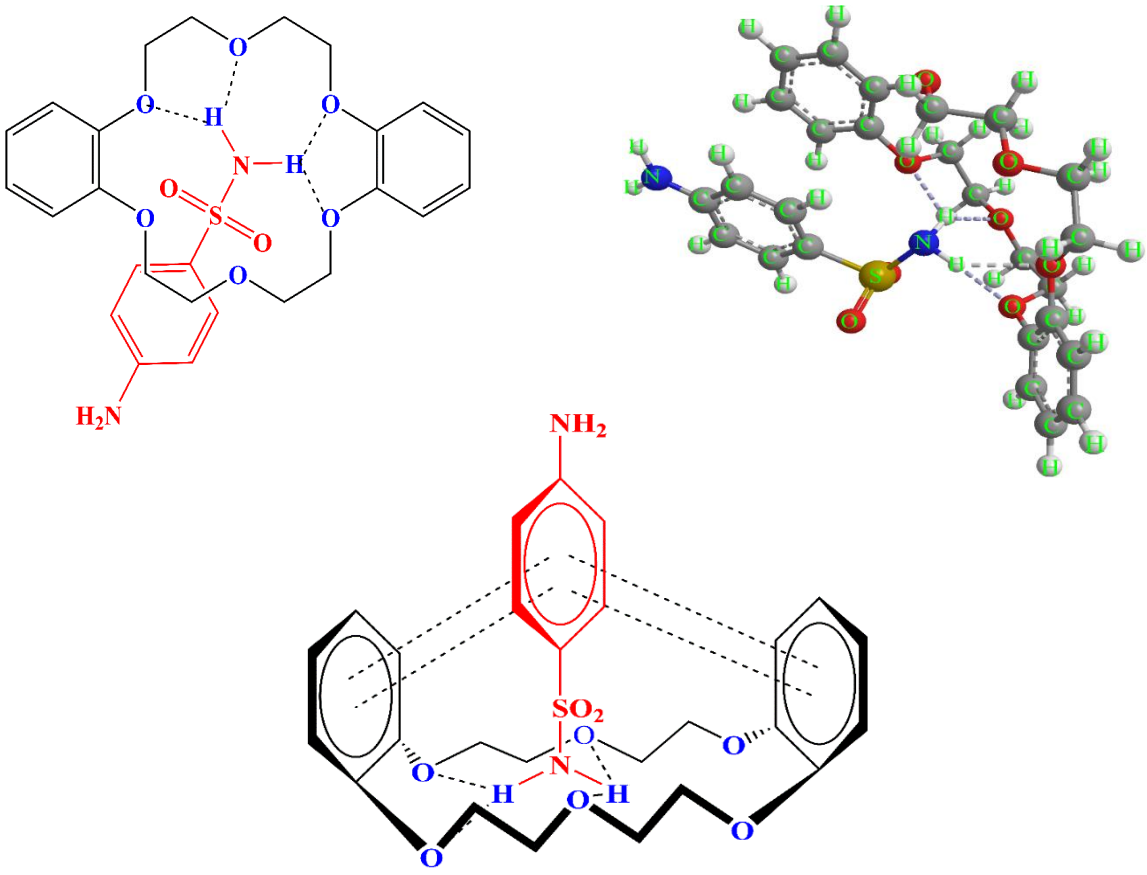

Scheme VII.2c: Schematic presentation of complex formation between SA and DB18C6 and corresponding energy minimized structure of the complex.

VII.3.9 Association constant and Thermodynamic parameters

The stability constants (K_a) for 1:1 complexation were measured in ACN solution by UV-visible spectroscopy and are presented in **Table VII.12**.

Table VII.12: Values of Association constant (K_a) and free energy change (ΔG^0) of the three SA-CEs complexes.

	T/K[a]	K_a/ M^{-1}	ΔG^0/KJ mol^{-1}
Complex 1		541.88	-15.60
Complex 2	298.15	412.27	- 14.94
Complex 3		372.80	-14.67

[a] Standard uncertainties in temperature are: (T) = ±0.01 K.

UV–vis spectroscopy is a convenient and widely used method for the study of binding phenomena [44]. The sulfa drug absorbs light at different wavelengths in free and complexed states and the differences in the UV–vis spectra may suffice for the estimation of molecular recognition thermodynamics. In UV spectroscopic titration experiments, the addition of varying concentration of host molecules results in a gradual increase or decrease of characteristic absorptions of the guest molecules. The association constants of the supramolecular systems formed were calculated according to the modified Benesi-Hildebrand equation, Eq. (8) [45], (**Figure VII.11**)

$$\frac{1}{\Delta A} = \frac{1}{\Delta\varepsilon[SA]K_a}.\frac{1}{[CE]} + \frac{1}{\Delta\varepsilon[SA]} \qquad (8)$$

Where [CE] and [SA] refer to the total concentration of crown ether and SA respectively, Δϵ is the change in molar extinction coefficient between the free and complexed crown ether and ΔA denotes the absorption changes of SA on the addition of CEs. The values of K_a for each of the complexes were evaluated by dividing the intercept by the slope (**Table VII.13-VII.15**) of the straight line of the double reciprocal plot. The free energy change (ΔG), has been easily estimated from association constant by using following equation [46, 47]

$$\Delta G = -RT\ln K \qquad (9)$$

The ΔG values (**Table VII.12**) for all the three complexes are negative which indicates that the Complex formation process proceeds spontaneously at 298.15K. In all the complexes, H-bonding to the ether oxygen atoms is obviously responsible for complexation but either π-stacking or charge-transfer interactions (**Scheme VII.2**) also seem to have a minor contribution towards complexation. The stability constants for complex 3 is slightly lower than the corresponding value of complex 1 and complex 2 (**Table VII.12**) as the aromatic rings of the crown ether decrease the electron density of the adjacent oxygen atoms, and this seems to decrease the strength of any H-bonding in complex 3. Although complex 3 has the potential for π-stacking or charge transfer interactions which is absent in the complex 1 and complex 2 indicates that H-bonding bonding to the ether oxygen atoms is dominant here for the complexation.

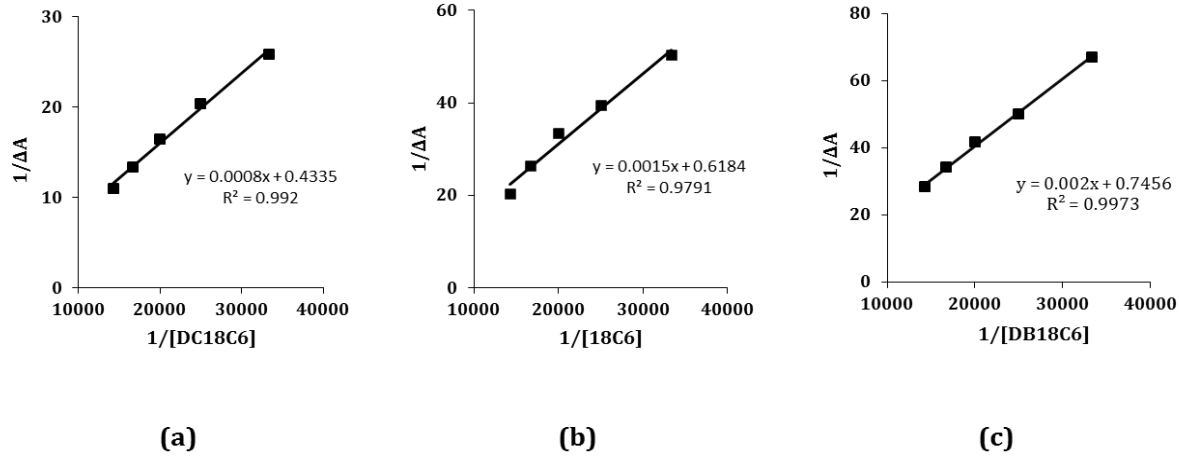

Figure VII.11: Benesi-Hildebrand double reciprocal plot for the effect of (a) DC18C6, (b) 18C6, (c) DB18C6 on the absorbance of Sulfa drug.

Table VII.13: Data for the Benesi-Hildebrand double reciprocal plot performed by UV-Vis spectroscopy for SA-DC18C6 system at T=298.15K.

[SA] /μM	[18C6] /μM	A_0	A	ΔA	1/[DC18C6] /M^{-1}	1/ΔA	Intercept	Slope	K_a /M^{-1}
50	30		1.10102	0.03868	33333	25.8531			
50	40		1.09072	0.04898	25000	20.4165			
50	50	1.13970	1.07887	0.06083	20000	16.4392	0.4335	0.0008	541.88
50	60		1.06496	0.07474	16667	13.3797			
50	70		1.04830	0.09140	14286	10.9409			

[a] Standard uncertainties in temperature are: (T) = ±0.01 K.

Table VII.14: Data for the Benesi-Hildebrand double reciprocal plot performed by UV-Vis spectroscopy for SA-18C6 system at T=298.15K.

[SA] /μM	[18C6] /μM	A_0	A	ΔA	1/[18C6] /M^{-1}	1/ΔA	Intercept	Slope	K_a /M^{-1}
50	30		1.11983	0.01987	33333	50.3271			
50	40		1.11434	0.02536	25000	39.4322			
50	50	1.13970	1.10973	0.02997	20000	33.3667	0.6184	0.0015	412.27
50	60		1.10165	0.03805	16667	26.2812			
50	70		1.09040	0.04930	14286	20.2840			

[a] Standard uncertainties in temperature are: (T) = ±0.01 K.

Table VII.15: Data for the Benesi-Hildebrand double reciprocal plot performed by UV-Vis spectroscopy for SA-DB18C6 system at T=298.15K.

[SA] /μM	[18C6] /μM	A_0	A	ΔA	1/[DB18C6] /M^{-1}	1/ΔA	Intercept	Slope	K_a /M^{-1}
50	30		1.15464	0.01494	33333	66.9344			
50	40		1.15971	0.02001	25000	49.9750			
50	50	1.13970	1.16372	0.02402	20000	41.6319	0.7456	0.0020	372.80
50	60		1.16887	0.02917	16667	34.2818			
50	70		1.17509	0.03539	14286	28.2565			

[a] Standard uncertainties in temperature are: (T) = ±0.01 K.

VII.4. CONCLUSION

The formation of three complexes of sulfa drug with several crown ethers in ACN have been investigated with the help of above mentioned spectroscopic and physicochemical studies. ^{1}H NMR data confirms the complex formation and the Job plot suggests the formation of complexes with 1:1 stoichiometry. The interaction of sulfa drug with crown ethers in the solution have been interpreted by density, viscosity, refractive index measurements. These measurements provide valuable information on ion-solvent and ion-ion interactions of the complexes in solutions. The formation constants are found highest for complex 2, then complex 1 and then complex 3 which indicates that SA form most stable complex with DC18C6 compared to other complexes. The probable structures of the three complexes of sulfa drug with crown ethers have been proposed by the above mentioned studies.

In this work we have found that the studied complexes are mainly stabilised by hydrogen bonds, and π-stacking play only a secondary role in case of complex 3 i.e complex of benzene substituted crown ether. The 1:1 complexation of the sulfa drug by different crown ethers proceeds spontaneously ($\Delta G^0 < 0$). The roles of guest SA has been established in directing the formation of supramolecular architectures between crown ether and $-NH_2$ group of $-SO_2NH_2$ in SA by host–guest hydrogen-bonding interactions. Here the present work helps to understand the vital role of $-NH_2$ group in the design and construction of supramolecular host–guest materials. These results are also significant for other host–guest systems. However, with the knowledge acquired from the solution chemistry of SA-Crown complexes, we believe that the scope and future prospect of this type of studies with other supramolecules are also a promising preposition.